From Five- to Six-Membered Rings: 3,4-Diarylquinolinone as Lead for Novel p38MAP Kinase Inhibitors

Christian Peifer,*,† Katrin Kinkel,† Mohammed Abadleh,† Dieter Schollmeyer,‡ and Stefan Laufer*,†

Institute of Pharmacy, Department of Pharmaceutical and Medicinal Chemistry, Eberhard-Karls-University Tübingen, Auf der Morgenstelle 8/B, D-72076 Tübingen, and Department of Organic Chemistry, Johannes Gutenberg-University Mainz, Duesbergweg 10-14, D-55099 Mainz, Germany

Received September 20, 2006

In this study we describe the design, synthesis, and biological evaluation of 3-(4-fluorophenyl)-4-pyridin-4-ylquinoline-2(1*H*)-one (**5**) as a new inhibitor of MAPK with a p38αMAPK IC_{50} of 1.8 μM. By keeping the common vicinal pyridine/4-F-phenyl pharmacophore, such as in prototypical imidazole **20** or isoxazole **13** but in **5** connected to the six-membered quinoline core, we were particularly interested in comparing biological activity, details of molecular geometry, and different binding modes of these compounds. Compounds **20** and **13** were active both in the p38α- and JNK3-assay, whereas **5** was selective for p38α, with no JNK3 inhibition. By comparing the X-ray structures of the compounds, we found a significantly larger distance between the pyridine and the 4-F-phenyl moiety in five-membered core structures relevant for ligand−protein interactions. Molecular modeling studies support the results based on differences in the ATP pockets of p38α and JNK3. Because most five-membered core based p38α inhibitors show also activity for JNK3, compound **5** is an interesting lead for selective p38α inhibitors.

Introduction

Protein Kinases as Drug Targets. Protein kinases (PKs[a]) are currently among the most important target classes for drug development as they regulate signal transduction by phosphorylating tyrosine, threonine, and serine residues in key proteins involved in signal pathways featuring relevance in many diseases.[1] Because PKs comprise 22% of the druggable genome, numerous opportunities for inhibitors arise to achieve promising treatments of severe diseases such as in oncology, diabetes, and inflammation.[2] Because all PKs use ATP as cofactor, they share a highly conserved ATP binding pocket, which is the molecular binding site of most inhibitors. The seminal work of Manning et al. has defined and categorized the "human kinome" space, consisting of 518 protein kinases that carry out the phosphorylation of proteins at 250 000 or more sites.[3−5] Thus, for drug candidates interfering with PKs, their range of specifity within the kinome is a key question, and a robust evaluation of potency and selectivity is an essential part of drug discovery.[6] However, it seems to be difficult to develop selective inhibitors, and currently there is an ongoing discussion whether a concept of single-targeting, group-targeting, multi-targeting, or even promiscous inhibitors across kinase space result in therapeutic benefit.[7,8] Besides malignant diseases, inhibitors of PKs are developed particularly as drugs against chronic inflammatory diseases such as rheumatoid arthritis (RA) and inflammatory bowel disease involving cytokine signaling pathways and mitogen-activated protein kinases (MAPKs) as drug targets therein.[9,11] In cancer therapy, multikinase targeting drugs with clinical efficacy but also side effects to be expected may be rather acceptable. In contrast, for PK inhibitors as anti-inflammatory drugs, the selectivity for a defined target within the kinome (and beyond[10]) will be key.

MAPKs and Inflammation. Therapeutic inhibition in cytokine signaling systems like IL-1β and TNF-α by small molecule ATP-competitive PKs inhibitors results in clinical benefit. These signal pathways provide a number of possibilities for the development of such small molecular agents and particularly MAPKs as validated targets have become widely accepted.[9] The well-characterized MAPKs are a group of protein kinases that play an essential role in signal transduction by modulating gene transcription in the nucleus in response to stresses in the cellular environment as well as in intracellular communication. In humans, there are at least 11 members of the MAPK superfamily that can be divided into six groups: extracellular signal-regulated protein kinases (ERK1 and ERK2); c-Jun N-terminal kinases (JNK1, JNK2, JNK3); p38s (p38-alpha, p38-beta, p38-gamma, p38-delta); ERK5 (ERK5); ERK3s (ERK3, p97-MAPK, ERK4); and ERK7s (ERK7, ERK8). Stimulation of MAPKs in each case in response to different extracellular stimuli lead to separate signal transduction pathways and specific phosphorylation of substrate proteins. Among the family of MAPKs, especially p38-alpha MAPK (p38α) and JNK3 are promising targets for drug development.[11] Both enzymes share the activation by certain cytokines, mitogens, osmotic stress, and ultraviolet irradiation through a complex upstream signal pathway and are most probably controlled by distinct intracellular complexes of multiple signaling proteins.[12] Among the MAPK, the ERKs function in the control of cell division, and inhibitors of these enzymes have potential as anticancer agents. The JNKs are critical regulators of transcription, and JNK inhibitors may be effective in the control of RA and neuronal inflammation diseases. The p38 MAPKs are mainly activated by inflammatory cytokines and environmental stresses and may contribute to asthma and diseases associated with autoimmunity.[13] Thus, MAPKs are involved in different tissues and the control of diverse physiological processes therein, and inhibition of multiple MAPKs could lead to potential side

* To whom correspondence should be addressed. Tel.: 0049(0)-70712975278 (C.P. and S.L.). Fax: 0049(0)7071295037 (C.P. and S.L.). E-mail: christian.peifer@uni-tuebingen.de (C.P.); stefan.laufer@uni-tuebingen.de (S.L.).

† Eberhard-Karls-University Tübingen.

‡ Johannes Gutenberg-University Mainz.

[a] Abbreviations: MAPKs, mitogen-activated protein kinases; JNK, c-Jun N-terminal kinase; PK, protein kinase; RA, rheumatoid arthritis; ERK, extracellular signal-regulated protein kinase; HPI, hydrophobic pocket I; HRII, hydrophobic region II.

10.1021/jm061097o CCC: $37.00
Published on Web 02/27/2007

Scheme 1. Left: Original Lead Compound **19** Showing the Central Pyridine/Fluorophenyl Pharmacophore. Right: Schematic Representation of p38α MAP Kinase ATP Binding Pocket[a]

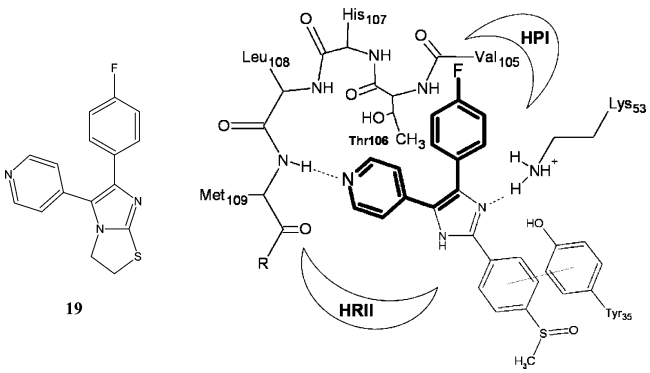

[a] Important interactions between ligand **20** and backbone amino acids are shown. The essential pharmacophore of the inhibitor is highlighted and the pyridine/fluorophenyl clasping around residue Thr106. HPI: hydrophobic pocket I. HRII: hydrophobic region II, solvent accessible.

effect profiles on immune and inflammatory systems. In particular, JNK3 and p38α have different downstream substrates in signaling pathways, and JNK3 is expressed also in neuronal cells. Thus, separation of p38α- and JNK3-inhibition (with selectivity over other kinases) and, therefore, dissection of the signaling pathways by small molecule inhibitors may be important requirements for the use in defined treatments.

Besides the approach to directly inhibiting kinases such as p38α and JNK3 at the level of MAPK, another strategy is to targeting upstream signaling proteins such as TAK1 or RIP2 (receptor-interacting kinase 2).[14] However, both concepts have pros and cons, and clinical efficacy will answer the question in each case which is more successful.

Inhibitors of p38 MAPK and JNK3. Originally developed from the early lead **19** (Scheme 1),[16a] the 1st generation p38 MAPK inhibitors were structurally related to the prototypical pyridinyl imidazole **20**. The central pharmacophore consists of a vicinal pyridine/fluorophenyl system, and to date, a huge number of inhibitors fulfilling this concept have been advanced into clinical trials.[15]

Crystallographic data demonstrate that **20** binds in the ATP binding site of p38α (Scheme 1).[16b] In detail, the pyridine ring nitrogen is accepting a hydrogen bond from the backbone NH of Met109 in the Hinge region. Vicinal to this interaction site, the 4-fluorophenyl moiety occupies the "hydrophobic pocket I" (HPI, consisting of Ala51, Lys53, Leu75, Ile84, Leu86, Leu104, Val105, and Thr106) causing selectivity of vicinal pyridine/fluorophenyl inhibitors for MAPK over other PKs.

Chart 1. Sample Compounds with Vicinal Pyridine/Fluorophenyl Pharmacophore Connected to Five- and Six-Membered Core Structures

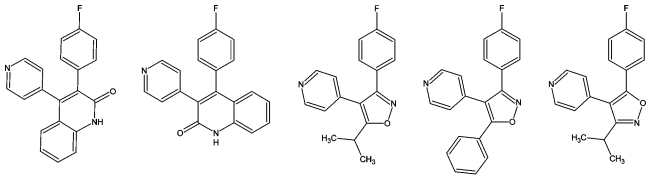

5 **10** **13** **15** **16**

Additional ligand−p38α interactions can be detected such as hydrogen bonding toward the core system from Lys53 and Tyr35 $\pi-\pi$ stacking with the phenyl system.

The binding mode of **20** shows the ligand not interfering with "hydrophobic region II". Thus, optimization of inhibitors to address HRII had been accomplished successfully mainly by introducing lipophilic substituents to the pyridine moiety such as phenylethylamine.[17] Furthermore, the nature of the core heterocycle and of the substituents has been varied extensively, mainly to enhance activity and selectivity.[18]

Most inhibitors of vicinal pyridine/fluorophenyl series contain the pharmacophore connected to a five-membered ring, which usually provides additional interactions to the protein such as prototypically compound **20** with imidazole accepting a H bond from Lys53 (Scheme 1).

In this study, maintaining the pyridine/fluorophenyl pharmacophore but connecting to a bicyclic six-membered ring, we designed 3-(4-fluorophenyl)-4-pyridin-4-ylquinoline-2(*1H*)-one (**5**, Chart 1) as a novel inhibitor of MAPK. To accept a H-bond from Lys53, and if applicable to address a H-bond to Asp168, the lactam moiety was considered to be favorable (Figure 1). The aromatic system of the quinoline moiety was supposed to be orientated to HRII and to provide options for further structural modifications. In fact, molecular modeling studies showed **5** to possess a reasonable binding mode in the ATP binding pocket of p38α (Figure 1).

Results and Discussion

Motivated by the binding mode, compound **5** was synthesized and an IC_{50} of 1.8 μM in the p38 in vitro assay was determined, strongly supporting the calculated ligand−protein interactions. Furthermore, to verify our hypothesis, we synthesized and subsequently evaluated compound **10** (Chart 1) as a regioisomer of **5**. Although **10** containing the vicinal pyridine/fluorophenyl pharmacophore, for binding in the described orientation as the regioisomer **5**, the bulky aromatic system of the quinoline moiety needs to be situated upside down, but "in silico" causing a clash with Lys53. Secondary, the above-mentioned H-bonding of the

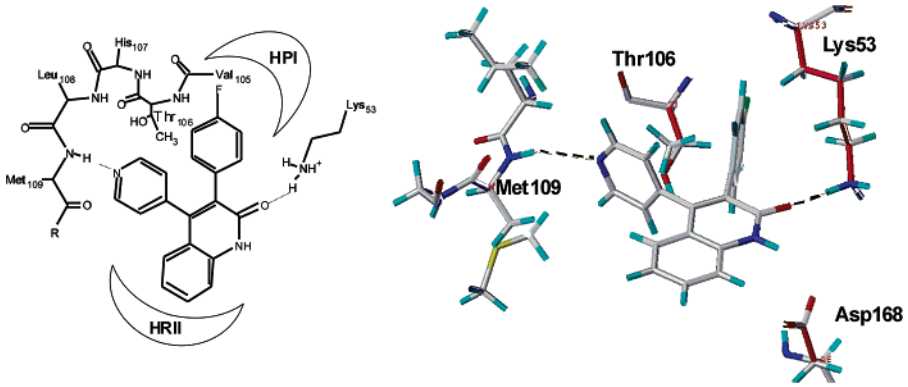

Figure 1. Schematic and modeled binding mode of **5** in the ATP binding pocket of p38α. Key residues and H-bond interactions are shown.

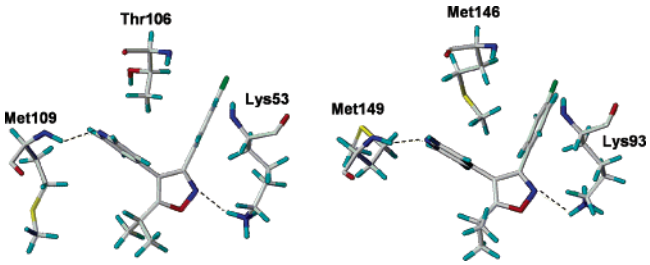

Figure 2. Modeled binding mode of **13** in the ATP binding pocket of p38α (left) and JNK3 (right). Key residues and H-bond interactions are shown.

Table 1. Overlay and Differences in ATP Binding Sites between Highly Homologous Protein Kinases JNK3 (Deep Blue) and p38α (Cyan)[a]

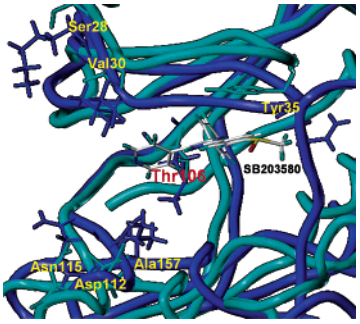

sequence # JNK3		sequence # p38α	
68	Lys	28	Ser
70	Ile	30	Val
75	Gln	35	Tyr
146	Met	106	Thr
152	Asn	112	Asp
155	Gln	115	Asn
196	Val	157	Ala

[a] Key residues Thr106/p38α and Met146/JNK3, presumably relevant for vicinal pyridine/fluorophenyl pharmacophore interaction, are highlighted. The numbering scheme of residues in yellow belongs to p38α (pdb code 1a9u, with the original based binding mode of **20**, white) and corresponding residues in JNK3 (pdb code 1pmn) are shown in deep blue without numbering for clarity.

lactam system to Lys53/Asp168 should be prevented. In fact, lack of p38α activity goes parallel with loss of a rational modeled binding mode of **10** in the ATP binding site of p38α. These findings support the discussed assumptions of ligand−p38α interactions for compound **5**. In addition, **5** (and **10)** was found to have no significant inhibitory activity to the closely related JNK3 (**5** @ 100 μM = 6% inhibition of JNK3) and no reasonable binding mode in the ATP pocket of JNK3 could be modeled. In contrast to these results, several pyridine/fluorophenyl-based inhibitors, for example, **20**, were reported to inhibit both p38α and JNK3.[19] Having successfully designed **5** as a new inhibitor of p38α with selectivity over JNK3, we were particularly interested if molecular geometry of the pyridine/fluorophenyl system due to connection to a 5- or 6-membered core influences the compound's activity to the highly homologous kinases p38α and JNK3.

To address this goal, we determined crystal structures by X-ray analysis of 6-membered ring isomer compounds **5**/**10** and of 5-membered ring compounds **13**/**16** (Chart 1) developed in our lab as dual p38α/JNK3 inhibitors (**13** p38α IC_{50} = 0.45 μM; JNK3 IC_{50} = 0.54 μM; **16** p38α IC_{50} = 2.2 μM; JNK3 IC_{50} = 3.5 μM). Compound **13** was chosen as useful for comparison due to related pharmacophore features and because activity for p38α of **13** matches activity of **5** (IC_{50} = 1.8 μM).

Table 2. In Vitro Activity for p38α[24]/JNK3[25] (± Standard Deviation, n = 6) and Details of Molecular Geometry for Compounds with Vicinal Pyridine/Fluorophenyl Pharmacophore Connected to Five- and Six-Membered Core Structures

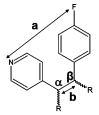

#	structure	p38α IC_{50} [μM]	JNK3 IC_{50} [μM]	a [Å]	b [Å]	α [°]	β [°]
5		1.80 (±0.05)	6% inhibition @100 μM (±0.07)	6.58	1.36	120.1	123.4
10		>10	>10	6.89	1.37	123.0	121.6
13		0.45 (±0.042)	0.54 (±0.008)	7.96	1.43	129.9	130.0
16		2.20 (±0.03)	3.50 (±0.01)	8.14	1.36	129.7	134.6
17		5.1 (±0.01)	28.50 (±0.02)	7.21[d]	1.40[d]	124.5[d]	125.6[d]
20	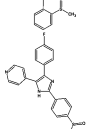	0.03 (0.01-0.05)[a]	0.79 (0.2-0.80)[a]	8.28	1.49	131.5	131.4
21	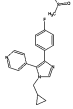	0.16[b]	nd[c]	7.84	1.50	127.8	129.2

[a] Range of IC_{50} values from ref 18. [b] See ref 16. [c] nd = not determined. [d] Calculated based on minimization by force field.

In this context, isoxazole **15** possessing a phenyl moiety (instead of isopropyl in analogue **13)** inhibits p38α with an IC_{50} of 12 μM, indicating consistent lipophilic interactions to HRII. Interestingly, compound **16** (4-[5-(4-fluorophenyl)-3-isopropylisoxazol-4-yl]pyridine) as an isomer of **13** (4-[3-(4-fluorophenyl)-5-isopropylisoxazol-4-yl]pyridine) was about 10-fold less active both in the p38α and JNK3 assay. Thus, **13**, with the isoxazole nitrogen situated close to the 4-F-phenyl position to accept the H bond from Lys53/p38α and Lys93/JNK3, respectively, indicates that the isoxazole nitrogen at this position is important for ligand−protein interactions in these enzymes.

A binding mode for **13** was modeled in the ATP site of p38α, showing a comparable orientation of the vicinal pyridine/fluorophenyl pharmacophore as **5** with accepting H-bonds both from Met109 by pyridine nitrogen as well as from quite flexible Lys53 by isoxazole nitrogen and the isopropyl moiety situated in the HRII (Figure 2). Accordingly to the in vitro activity of **13** in JNK3, a binding mode was modeled for this enzyme, too. Significantly comparable to p38α, the pyridine N is accepting a H bond from Met149, the fluorophenyl is situated in HPI, the isoxazole N is accepting a H bond from Lys 93, and the isopropyl moiety is located in HRII. The two aromatic residues clasp around gatekeeper residue Thr106 in p38α and Met146 in JNK3, which is more spacious in this enzyme (Figure 2).

Taken together, **13** and **5** show a comparable binding mode and activity for p38α but not for JNK3. Thus, we evaluated molecular details of these compounds concerning ligand−protein interactions to the highly homologous proteins p38α and JNK3.

Analogy of p38α and JNK3. In spite of the fact that MAPKs share highly conserved ATP binding pockets, specific structural

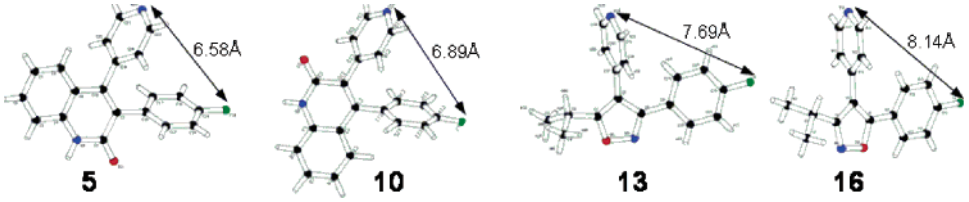

Figure 3. Schakal plot of molecular structures determined by X-ray crystallography of compounds **5**, **10**, **13**, and **16**, showing the numbering scheme and the pyridine/4-F-phenyl distance.

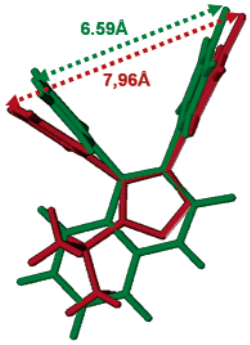

Figure 4. Overlay of pose in the ATP binding pocket of p38α for **5** (green) and **13** (red) showing different inner width of the vicinal pyridine/fluorophenyl pharmacophore.

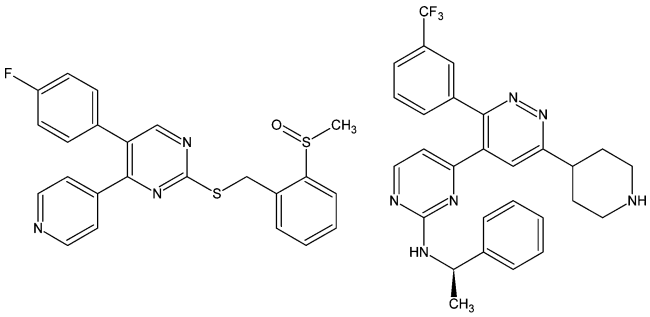

Figure 5. Six-membered core MAPK inhibitors pyrimidine **17** and pyrimidinylpyridazine **18**.

differences in p38α and JNK3 (Table 1) can be found that are able to cause selectivity for ligands.[19]

Concerning relevant interaction sites for the unsubstituted vicinal pyridine/fluorophenyl pharmacophore in the hinge region, actually in contrast to gatekeepr Thr106, in p38α at the same position in JNK3 the more spacious residue Met146 is situated. Considering the binding mode of inhibitors exhibiting the vicinal pyridine/fluorophenyl pharmacophore, the two aromatic systems clasp in each case around this residue.[16]

This prompted us to investigate the influence of orientation and dimension of the two aromatic moieties depending on the 5- or 6-membered core system to which they are connected in light of design for inhibitors of p38α and JNK3 (Table 2). For clarity, in this study data for compounds **5**,[20] **10**,[21] **13**,[22] and **16**[23] have been evaluated precisely by X-ray crystallography (Figure 3), whereas **20** and **21** were analyzed from PDB ligand−protein structures. Data for compound **17** was calculated by semiempirical force field minimization.

The exocyclic bond angle by which the vicinal pyridine and fluorophenyl moiety is fixed to the core cycle has a crucial bearing on the distance between the aromatic moieties that are orientated around key residue Thr106/p38α and Met146/JNK3, respectively (Table 2). For **5** (six-membered core), we determined a pyridine/4-F-phenyl (tip to tip) distance of 6.59 Å and for **13** (five-membered core), a significant larger distance of 7.96 Å (Figure 4). The expanded dimension of amino acid Met146/JNK3 (volume 3970.01 ± 34.28 Å^3) compared to Thr106/p38α (volume 3687.29 ± 30.65 Å^3), and at the same time, the more closed configuration of the pyridine/fluorophenyl system in **5** with 1.38 Å less inner width than in **13** (Figure 4) could prevent appropriate access to the binding interactions in JNK3 for **5**. In contrast to **5**, compound **13** fits both pockets due to more commodious molecular geometry and therefore inhibiting both kinases. Thus, due to the impact of this quinoline six-membered core, fixing the vicinal pyridine/fluorophenyl system activity for p38α but not for JNK3 results.

Six-Membered Heterocycles as MAPK Inhibitors. Pyrimidine derivatives with a six-membered scaffold for fixing the vicinal unsubstituted pyridine/fluorophenyl pharmacophore, such as compound **17** (Figure 5), have been developed in our lab.[26] Though possessing a six-membered scaffold, structural analysis of **17** revealed that the geometrical data is not comparable to **5** (Table 2). The pyrimidine core is fixing the pyridine/fluorophenyl pharmacophore with exocyclic bond angles of 124.5°/125.6° and a pyridine/4-F-phenyl (tip to tip) distance of 7.21 Å, which enables appropriate interaction of the pharmacophore to both key residues Thr106/p38α (IC_{50} p38α = 5.1 μM) and Met146/JNK3 (IC_{50} JNK3 = 28.5 μM). Although pyridinyl imidazoles are among the most potent inhibitors of MAPK, enlargment of the five-membered core heterocycle to analog pyrimidine was reported to lead to a substantial decrease of in vitro activity for p38α.[17] Pyrimidinylpyridazines developed at Merck are very potent p38α inhibitors, such as compound **18** (Figure 5) with an IC_{50} p38α = 0.15 nM.[27] However, **18** has been optimized and is not comparable to the SAR of unsubstituted pyridine/fluorophenyl compounds described in this study.

Five-Membered Heterocycles as MAPK Inhibitors. Furthermore, we evaluated the molecular geometry of vicinal unsubstituted pyridine/fluorophenyl compounds **20** (PDB code 1a9u[16]) and **21** (PDB code 1bmk[16]) at the basis of ligand−p38α complexes (Table 2). In these five-membered core ligands, comparable molecular geometry (exocyclic bond angles pyridine/4-F-phenyl distances) as in biologically active compound **13** can be found. For instance, in the **20**−p38α complex, the ligand is showing vicinal exocyclic bond angles at imidazole bearing pyridine and 4-F-phenyl ring of 131.5° and 131.4°, respectively. These data underline the influence concerning activity and protein−ligand interactions of the molecular geometry of the core cycle fixing the pyridine/4-F-phenyl pharmacophore.

Conclusions

In this study, we discovered compound **5** as a new inhibitor of p38αMAPK, with an IC_{50} of 1.8 μM and with selectivity over the closely related JNK3. Due to the impact of the quinoline six-membered core, fixing the vicinal pyridine/4-F-phenyl system activity for p38α but not for JNK3 results. In contrast, compounds **13** and **16** possessing the five-membered isoxazole core were both found to inhibit p38α as well as JNK3. Molecular

Scheme 2. Synthesis of Compound **5**[a]

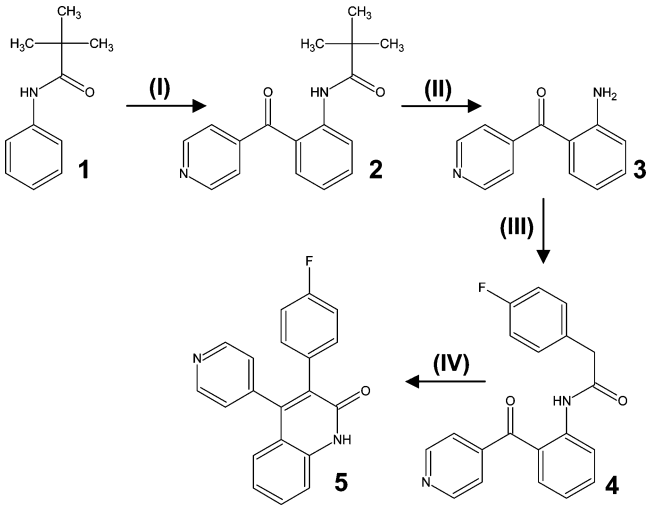

[a] Reagents and conditions: **(I)** (a) 0 °C THF/BuLi 2.7 M, 2 h; (b) pyridylcarboxaldehyde; (c) 0 °C acetone/Jone's oxidation $K_2Cr_2O_7$, 1 h; **(II)** ethanol/HCl reflux, 72 h; **(III)** dissolve in DCM/pyridine, then addition of 4-fluorophenylacetyl chloride in DCM, rt, 12 h; **(IV)** ethanol/KOH reflux, 2 h.

modeling supports these data showing important roles of key residues Thr106/p38α and Met146/JNK3. Because most five-membered core based p38α inhibitors show also activity for JNK3, compound **5** is an interesting lead for the development of selective p38α inhibitors.

Chemistry

Among the number of synthetic methods for preparing 3,4-diarylquinoline-2(1*H*)-one derivatives[28,29] in this study the ring closure to form the quinolin-2(1*H*)-one moiety was achieved by a Knoevenagel reaction. Synthesis of compound **5** was achieved in four steps (Scheme 2). The pivaloyl moiety in **1** works as a "directed ortho-metalation" group by which lithiation of the aromatic moiety was achieved in the aniline-ortho position under mild conditions.[30] This intermediate was quenched by S_EAr reaction with pyridylcarboxaldehyde to gave the alcohol *N*-{2-[hydroxy(pyridin-4-yl)methyl]phenyl}-2,2-dimethylpropanamide as an intermediate, which was conveniently oxidized by Jone's reagent[31] to yield **2**. It is noteworthy that reaction of lithiated species of **1** with ethyl isonicotinate gave **2** directly but in significant lower yield with side products complicating further procedure. Furthermore, the metalation step was found to be very sensitive and, therefore, the lithiated species was not transferred to ethyl isonicotinate, which would have provided **2** without the need of an oxidation step. However, in this strategy, 73% yield of **2** via forming the alcohol followed by oxidation was sufficient. To remove the pivaloyl group, **2** was refluxed in ethanol/HCl for 72 h (**3**), which was subsequently acylated by 4-fluorophenylacetic acid chloride to yield amide **4**. Straightforward ring closure to final compound quinoline **5** by Knoevenagel[32] reaction in KOH/ethanol was achieved in high yield.

Synthesis of compound **10** was achieved in five steps by comparable strategy for the last step as for **5**. Initially, 2-aminobenzoic acid was amino-protected by TsCl to yield carbonic acid derivative **6**, which was reacted with PCl_5 to form the acid chloride. In this study, fluorobenzene was conveniently used as solvent for forming the acid chloride. Thus, by addition of the Lewis acid $AlCl_3$ to the reaction mixture, a one pot Friedel−Crafts-acylation was achieved to yield **7** (and **8** due to hydrolysis of the Ts moiety under the acidic conditions). The crude mixture was stirred in HCl for complete deprotection to yield compound **8**.

Scheme 3. Synthesis of Compound **10** (Regioisomer of **5**)[a]

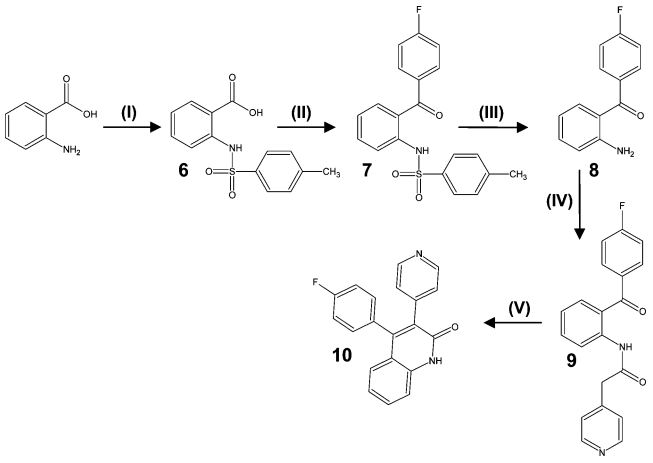

[a] Reagents and conditions: **(I)** TsCl/NaOH/H_2O, 12 h; **(II)** (a) fluorobenzole/PCl_5, heating for 30 min; (b) 0 °C/$AlCl_3$ in portions, rt, 1 h; **(III)** HCl 0 °C; **(IV)** DCM/pyridine, add 4-pyridylacetyl chloride in DCM, rt, 12 h; **(V)** NH_3, rt, 2 h.

Scheme 4. Synthesis of Compound **13**[a]

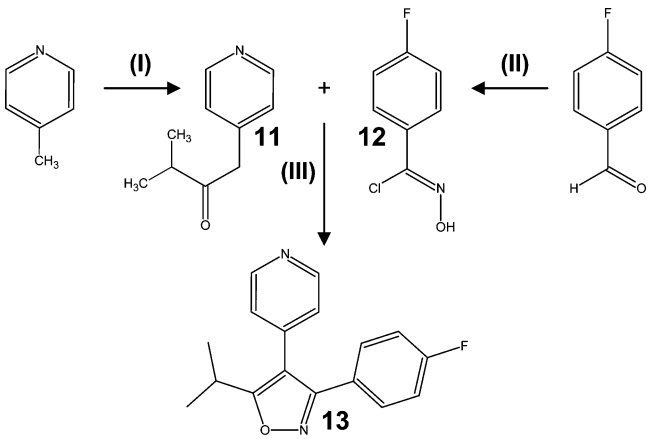

[a] Reagents and conditions: **(I)** (a) LDA/THF, −78 °C, 1 h; (b) isobutyraldehyde, 3 h; (c) Jone's oxidation, $K_2Cr_2O_7$/acetone, 0 °C, 3 h; **(II)** (a) hydroxylamine HCl/ethanol, 50% NaOH, rt, 2 h; (b) NCS/DMF, rt, 2 h; **(III)** triethylamine/ethanol, reflux, 16 h.

Pyridin-4-ylacetic acid HCl was reacted with PCl_5 to yield the corresponding acid chloride, which was obtained in almost quantitative yield. Pyridin-4-ylacetic acid chloride was used without further purification for aminoacylation of **8** and **9**. It is noteworthy that for preparation of pyridin-4-ylacetic acid chloride only PCl_5 was successful and other common reagents such as thionylchloride gave only red tars. The Knoevenagel reaction for formation of 4-(4-fluorophenyl)-3-pyridin-4-ylquinoline-2(1*H*)-one **10** was conveniently performed by addition of ammonia (Scheme 3).[32]

Isoxazole **13** was prepared in a one-pot synthesis by refluxing **11** (3-methyl-1-(pyridine-4-yl)butan-2-one) and **12** (4-fluorobenzoyl chloride oxime) with triethylamine ethanol (Scheme 4).

For synthesis of **15** and **16**, the expedient precursor **14** was used (Scheme 5), which was prepared in a modified procedure according to the literature.[33] Compound **14** was transferred to 1-(4-fluorophenyl)-2-(4-pyridine)ethanone oxime, which gave isoxazole **15** by reaction with hydroxybenzenecarboximidoyl chloride and triethylamine. Compound **16** was prepared in a one-pot synthesis procedure (modified according to the literature[34]) by deprotonating **14** with LDA, followed by isobutyryl

Scheme 5. Synthesis of **15** and **16** from Precursor **14**[a]

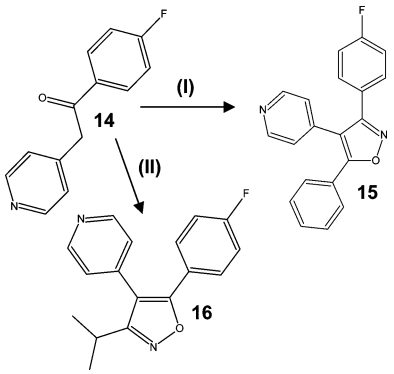

[a] Reagents and conditions: **(I)** (a) sodium acetate/hydroxylamine, HCl/ethanol, reflux, 1.5 h; (b) triethylamine/DCM, 0 °C, 1 h, *N*-hydroxybenzenecarboximidoyl chloride, 0 °C to rt, 12 h; **(II)** (a) LDA/THF, −78 °C, 1 h; (b) isobutyryl chloride oxime/THF.

chloride oxime, which gave 4-[5-(4-fluorophenyl)-3-isopropylisoxazol-4-yl]pyridine **16** as an isomer of **13**.

Experimental Section

Chemistry. Infrared spectra were recorded on a "Perkin-Elmer Spectrum one" infrared spectrophotometer. ^{1}H (200 MHz, digital resolution 0.3768 Hz) and ^{13}C (50 MHz, digital resolution 1.1299 Hz) NMR were recorded on a Bruker AC 200. The data are reported as follows: chemical shift in ppm from Me_4Si as external standard, multiplicity and coupling constant (Hz). GC/MS was performed on a HP6890 Series System. EI mass spectra were recorded on a Varian MAT 311A (70 eV) and FD mass spectra on a MAT-95 (Finnigan). For clarity, only the highest measured signal is given for FD mass spectra. Elemental analyses were performed on an Elemental Analyzer Carlo Erba Strumentazione and agreed with the calculated data within ± 0.4 unless otherwise stated. Melting points/decomposition temperatures were determined on a Büchi apparatus, according to Dr. Tottoli, and are uncorrected. X-ray structure determination was performed on a CAD4-Enraf-Nonius using Cu K_α radiation with graphitmonochromator. Where appropriate, column chromatography was performed for crude precursors with Merck silica gel 60 (0.063−0.200 mm) or Acros organics silica gel (0.060−0.200 mm; pore diameter ca. 60 nm). Column chromatography for test compounds was performed using a La-Flash-System (VWR) with Merck silica gel 60 (0.015−0.040 mm) or RP18 columns. The progress of the reactions was monitored by thin-layer chromatography (TLC) performed with Merck silica gel 60 F-245 plates. Where necessary, reactions were carried out in a nitrogen atmosphere using 4 Å molecular sieves. All reagents and solvents were obtained from commercial sources and used as received (THF was used after distillation over K/benzophenone). Reagents were purchased from Sigma-Aldrich Chemie, Steinheim, Germany; Lancaster Synthesis, Mühlheim, Germany; or Acros, Nidderau, Germany.

***N*-(2-Isonicotinoylphenyl)-2,2-dimethylpropanamide (2). (a)** An amount equal to 1063 mg (6 mmol) of 2,2-dimethyl-*N*-phenylpropanamide (**1**, *N*-pivaloylaniline) was dissolved in dry THF under an argon athmosphere and cooled to 0 °C. Over 30 min, 4.5 mL of a solution of *n*-BuLi (2.7 M in heptane) was added dropwise to keep the temperature below 5 °C (it is noteworthy to use absolute dry THF and 2.7 M BuLi, because the reaction is very sensitive!). By addition of 3 mL of BuLi a slight turbidity was developed. After stirring 2 h in the ice bath, 1070 mg (10 mmol) of isonicotinaldehyde (pyridincarboxaldehyde) in 5 mL of THF was added dropwise to keep the temperature below 5 °C. A deep red color occurred immediately, and after stirring overnight, a white precipitate was formed. The reaction was quenched by the addition of ice/water and extracted twice with 200 mL of ethyl acetate. The organic phase was separated and evaporated under vacuum to about 20 mL. A short silica gel column was run (mobile phase ethyl acetate 5/hexanes 1) to recover unreacted **1** and isonicotinaldehyde. Removal of solvents under vacuum yielded **2** as a colorless thick oil, which gave white crystals by the addition of diethyl ether and slow evaporation. Yield 73% (1.25 g, 4.4 mmol). The compound was immediately used for oxidation. A sample of *N*-{2-[hydroxy-(pyridin-4-yl)methyl]phenyl}-2,2-dimethylpropanamide was analyzed: GC/MS rt = 28.7 min. EI-MS (*m*/*z*): 284 (M^+). ^{1}H NMR ($CDCl_3$, 200 MHz, ppm): δ 1.0 (s, 9H, CH_3), 5.8 (s, 1H, CH), 7.1 (d, 2H, CHar), 7.2 (m, 3H, CHar), 8.1 (d, 1H, CHar), 8.2 (d, 2H, CHar), 9.2 (s, 1H, NH).

(b) Jone's Oxidation. Preparation of Jone's reagent: 2 mL of concentrated sulfuric acid were added to 2 g of sodium dichromate dihydrate dissolved in 6 mL of water to form a carrot orange solution. To a solution of *N*-{2-[hydroxy(pyridin-4-yl)methyl]-phenyl}-2,2-dimethylpropanamide (1.1 g) in acetone at 0 °C, the Jone's reagent was added dropwise until the color remains red. After stirring for 1 h, the reaction control by TLC showed complete oxidation. The whole mixture was extracted over a short column of silica gel by 300 mL of ethyl acetate to remove chromine salts. The green-yellow organic phase was washed with brine, separated, and dried over Na_2SO_4. Evaporation of solvents under vacuum gave a brown oil. The crude compound was used for deprotection. A purified sample of **2** was analyzed: GC/MS rt = 24.3 min; EI-MS (*m*/*z*) 282 (M^+). ^{1}H NMR ($CDCl_3$, 200 MHz, ppm): δ 1.4 (s, 9H, CH_3), 7.1 (t, 1H, CHar), 7.5 (d, 3H, CHar), 7.6 (t, 1H, CHar), 8.8 (m, 3H, CHar), 11.4 (s, 1H, NH).

(2-Aminophenyl)(pyridin-4-yl)methanone (3). Crude compound **2** (0.8 g/2.84 mmol) was dissolved in 100 mL of ethanol/10 mL of concd HCl and refluxed for 72 h. The progress of the reaction was monitored by GC/MS. The reaction mixture was cooled in an ice bath and brought to pH 10 by addition of NaOH solution and extracted with diethyl ether. Drying over Na_2SO_4 and evaporation of solvents gave a yellow solid. Yield 85.9% (484 mg, 2.44 mmol), which was recrystallized from ethanol; mp = 163 °C; GC/MS rt = 17.9 min; EI-MS (*m*/*z*) 198 (M^+). ^{1}H NMR ($CDCl_3$, 200 MHz, ppm): δ 6.3 (br s, 2H, NH), 6.6 (t, 1H, CHar), 6.7 (d, 1H, CHar), 7.3 (d, 2H, CHar), 7.4 (d, 2H, CHar), 8.8 (d, 2H, CHar).

2-(4-Fluorophenyl)-*N*-(2-isonicotinoylphenyl)acetamide (4). A dry 100 mL three-neck round-bottom flask with septum and bubble counter was equipped with 154 mg (1 mmol) of (4-fluorophenyl)-acetic acid and 210 mg (1 mmol) of PCl_5 in 4 mL of DCM and stirred overnight. The reaction was then cooled to 0 °C under an argon athmosphere, and a solution of 200 mg (1 mmol) of **3** in 5 mL of dry DCM/100 mg of dry pyridine was added carefully. After stirring overnight, water and ammonia were added, and the mixture was extracted with DCM to remain the water-phase citreous. The organic phase was separated, dried over Na_2SO_4, and evaporated. Yield 320 mg (0.96 mmol, 96%) as a light yellow oil; GC/MS rt = 42.86 min; EI-MS (*m*/*z*) 334 (M^+). ^{1}H NMR ($CDCl_3$, 200 MHz, ppm): δ 3.8 (s, 2H, CH_2), 7.1 (m, 3H, CHar), 7.3−7.5 (m, 5H, CHar), 7.6 (t, 1H, CHar), 8.7 (d, 1H, CHar), 8.8 (d, 2H, CHar), 11.0 (br s, 1H, NH).

3-(4-Fluorophenyl)-4-pyridin-4-ylquinoline-2(1*H*)-one (5). An amount equal to 300 mg (890 mmol) of compound **4** was dissolved in 100 mL of ethanol/50 mg of KOH and refluxed for 2 h. The progress of the reaction was monitored by TLC, which showed a spot of **6** with blue fluorescence at 366 nm. Purification of the reaction mixture by silica gel chromatography ethyl acetate 5/hexanes 1 gave **5** as a pale yellow solid. Yield 93% (260 mg, 83.4 mmol); mp = 352 °C; GC/MS analysis revealed no peak up to 53 min/300 °C. Syringe pump infusion ion trap analysis +c Full ms (*m*/*z*), 339.1 (Na^+ adduct of M^+); −c Full ms (*m*/*z*), 315.3 (M^-). ^{1}H NMR (DMSO-d_6, 200 MHz, ppm): δ 6.9−7.3 (m, 8H), 7.4−7.6 (m, 2H), 8.5 (d, 2H), 12.2 (br s, 1H, NH). Anal. ($C_{20}H_{13}FN_2O$) C, H, N.

Crystal structure of **5** has been proven by X-ray analysis: CAD4 Enraf Nonius, Cu Kα, SIR-92, SHELXL-97. Further details of the crystal structure analysis are available in references.[20]

2-{[(4-Methylphenyl)sulfonyl]amino}benzoic Acid (6). Amounts equal to 1.4 g of 2-aminobenzoic acid, 1.9 g of 4-methylbenzenesulfonyl chloride (TsCl), and 0.5 g of NaOH were stirred in 100

mL of H_2O overnight. The product was filtered, washed with water, dried, and recrystallized from diethyl ether. Yield 79%; mp = 212 °C; MS −c Full ms (*m*/*z*), 290.0 (M^-). ^{1}H NMR (DMSO-d_6, 200 MHz, ppm): δ 2.3 (s, 3H, CH_3), 7.1 (m, 1H, CHar), 7.3 (d, 2H, CHar), 7.5 (s, 2H, CHar), 7.7 (d, 2H, CHar), 7.9 (d, 1H, CHar), 11.1 (br s, 1H, NH).

***N*-[2-(4-Fluorobenzoyl)phenyl]-4-methylbenzenesulfonamide (7).** Compound **6** was reacted with fluorobenzene under Friedel−Crafts conditions: 5.84 g of **6**, 4.76 g of PCl_5, and 20 mL of fluorobenzene were refluxed until the solution became clear. The mixture was cooled in an ice bath, and after addition of 11.6 g of $AlCl_3$, the reaction was stirred for 1 h at 0 °C and then warmed to rt. A sample was extracted by ethyl acetate, purified, and analyzed. MS +c Full ms (*m*/*z*), 370.0 (M^+). ^{1}H NMR ($CDCl_3$, 200 MHz, ppm): δ 2.2 (s, 3H, CH_3), 7.0 (m, 5H, CHar), 7.3−7.5 (m, 5H, CHar), 7.53 (d, 1H, CHar), 7.8 (d, 1H, CHar), 9.80 (s, 1H, NH).

(2-Aminophenyl)(4-fluorophenyl)methanone (8). The crude mixture of **7** was poured on ice/50 mL of HCl and stirred for 1 h for complete deprotection. Ethyl acetate was added, and the organic phase was separated and dried over Na_2SO_4. Evaporation under vacuum gave a brown oil that was purified by column chromatography (ethyl acetate/hexanes 1/5) to yield a yellow oil (67%) of which bright yellow crystals were obtained by slow evaporation. GC/MS rt = 13.04 min; EI-MS (*m*/*z*) 215 (M^+). ^{1}H NMR ($CDCl_3$, 200 MHz, ppm): δ 6.0 (br s, 2H, NH), 6.6 (t, 1H), 6.7 (d, 1H), 7.1 (t, 2H), 7.3 (m, 1H), 7.4 (dd, 1H), 7.7 (m, 2H).

4-(4-Fluorophenyl)-3-pyridin-4-ylquinoline-2(1*H*)-one (10). Amounts equal to 175 mg (1 mmol) of pyridin-4-ylacetic acid hydrochloride and 210 mg of PCl_5 (1 mmol) were suspended in 4 mL of DCM and stirred overnight under a slight argon flow at rt. After cooling at 0 °C, a solution of 215 mg (1 mmol) of **8** and 100 mg of pyridine in 4 mL of DCM were added via septum, and the mixture was stirred for 12 h. Reaction progress was monitored as decreasing of **8** by TLC until this material disappeared to form compound **9**, which was immediately used for ring closure: 2 mL of ammonia was added, the mixture was stirred for 2 h, and the organic phase was separated and extracted by DCM over a short silica gel column. Evaporation gave a white solid, which was washed with diethyl ether to yield 74% of compound **10**; mp = 319 °C; MS +c Full ms (*m*/*z*) 317.0 (M^+); GC/MS rt = 45.73 min; EI-MS (*m*/*z*) 316 (M^+). ^{1}H NMR ($CDCl_3$, 200 MHz, ppm): δ 6.9−7.2 (m, 7H), 7.2 (m, 1H), 7.3 (d, 1H), 7.5 (m, 1H), 8.5 (ds, 2H), 12.0 (br s, 1H, NH). Anal. ($C_{20}H_{13}FN_2O$) C, H, N.

Crystal structure of **10** has been proven by X-ray analysis: CAD4 Enraf Nonius, Cu Kα, SIR-92, SHELXL-97. Further details of the crystal structure analysis are available in references.[21]

3-Methyl-1-pyridin-4-ylbutan-2-one (11). (a) Diisopropylamine (12.0 mmol) in 20 mL of THF was cooled to −78 °C, butyllithium (1.6 M, 1.1 equiv) was added dropwise, and the reaction mixture was stirred for 1 h at −78 °C. Picoline (11.0 mmol) in THF was added dropwise, and the color changed to yellow then became brown. The reaction was stirred for 1 h at −78, followed by addition of isobutyraldehyde (11.1 mmol) in THF and again stirred for 3 h at −78 °C, then allowed to stir to reach rt. Water (50 mL) was added carefully, and the mixture was extracted by ethyl acetate (200 mL). The organic phase was separated, dried over Na_2SO_4, and evaporated. The oily yellow product was purified by column chromatography using ethyl acetate 10/hexanes 1 to yield 3-methyl-1-(pyridine-4-yl)butan-2-ol. A sample was analyzed: MS +c Full ms (*m*/*z*) 166.2 (M^{+1}). ^{1}H NMR ($CDCl_3$, 200 MHz, ppm): δ 0.88 (s, 3H, CH_3), 0.92 (s, 3H, CH_3), 1.62 (m, 1H, CH), 2.5−2.65 (m, 2H, CH_2), 3.48 (m, 1H, CH), 4.44 (br s, 1H, OH), 7.0 (d, 2H, CHAr), 8.1 (d, 2H, CHAr). ^{13}C NMR ($CDCl_3$, 200 MHz, ppm): δ 17.3 (CH_3), 18.8 (CH_3), 33.7 (CH), 40.1 (CH_2), 77.1 (CH), 124.9 (CH), 148.7 (CH), 149.7 (C_q).

(b) Jone's Oxidation: 3-methyl-1-(pyridine-4-yl)butan-2-ol (1.2 mmol) was dissolved in 5 mL of acetone, the freshly prepared Jone's reagent (2 mL of concentrated sulfuric acid were added to 2 g of sodium dichromate dihydrate dissolved in 6 mL of water to form a carrot-orange solution) was dropped in intervals until the color changed from yellow to red brown, and the reaction mixture was allowed to stir for 2 h. Water was added, and the reaction was neutralized by NaOH. The mixture was extracted by ethyl acetate (200 mL), and the organic phase was separated, dried over Na_2SO_4, and evaporated to yield 52% of **11** as a pale yellow oil: MS +c Full ms (*m*/*z*) 164.2 (M^+). ^{1}H NMR ($CDCl_3$, 200 MHz, ppm): δ 1.0 (s, 3H, CH_3), 1.1 (s, 3H, CH), 2.6−2.8 (m, 1H, CH), 3.8 (s, 2H, CH_2), 7.1 (d, 2H, CHAr), 8.5 (d, 2H, CHAr). ^{13}C NMR ($CDCl_3$, 200 MHz, ppm): δ 18.0 (CH_3), 40.1 (CH), 46.2 (CH_2), 124.7 (CH), 143.2 (C_q), 149.7 (CH), 209.8 (CO).

4-Fluoro-*N*-hydroxybenzenecarboximidoyl Chloride (12). Compound **12** was prepared according to the literature with an optimized procedure in this study. (a) 4-Fluorobenzaldehyde (16 mmol) was dissolved in 25 mL of ethanol, 25 mL of water, and 40 g of ice. Hydroxylamine HCl (96 mmol) was added, followed by the dropwise addition of 55 mL of 50% NaOH. When the addition of NaOH was finished, the ice bath was removed, and the mixture was allowed to stir at rt for 2 h, yielding 15.1 mmol of 4-fluorobenzaldehyde oxime (94%). (b) The oxime was dissolved in 5 mL of DMF and stirred at rt, NCS (15.7 mmol) was added slowly by spatula, and the reaction was stirred at rt for 2 h. The reaction was quenched by adding water, and the mixture was extracted with diethyl ether (200 mL). The organic phase was washed with cold brine three times and separated, dried over Na_2SO_4, and evaporated. The residue was kept at 5 °C, where a white solid precipitated to yield 95% of **12**. ^{1}H NMR ($CDCl_3$, 200 MHz, ppm): δ 7.1 (m, 2H, CHAr), 7.82 (m, 2H, CHAr), 7.9 (br s, 1H, OH). Part of the compound was immediately used for the synthesis of **13**. It can be stored under argon at 7 °C.

4-[3-(4-Fluorophenyl)-5-isopropylisoxazol-4-yl]pyridine (13). Compound **11** (2.5 mmol) and 4.3 mmol of **12** were stirred in 10 mL of ethanol at room temperature. By addition of 1 mL of triethylamine, the color changed from yellow to deep orange then to brown. The reaction mixture was stirred 4 h at rt and then refluxed for 16 h. A saturated solution of NH_4Cl (50 mL) was added, and the mixture was extracted by ethyl acetate (200 mL). The organic phase was separated, dried over Na_2SO_4, and evaporated. The oily brown product was purified by column chromatography using ethyl acetate 10/hexanes 1 to yield 45% of **13**, which precipitated from ethanol as clear white crystals: mp = 144.0 °C. ^{1}H NMR ($CDCl_3$, 200 MHz, ppm): δ 1.3 (s, 3H, CH_3), 1.4 (s, 3H, CH_3), 3.1−3.2 (m, 1H, CH), 7.1 (m, 4H, CHAr), 7.3 (m, 2H, CHAr), 8.2 (d, 2H, CHAr). ^{13}C NMR ($CDCl_3$, 200 MHz, ppm): δ 20.9 (CH_3), 26.4 (CH), 111.6 (C_q), 115.5 (CH), 116.0 (CH), 124.5 (CH), 130.2 (CH), 130.4 (CH), 138.8 (C_q), 150.1 (CH), 159.9 (C_q), 161.0 (C_q), 165.9 (C_q), 175.3 (C_q). Anal. ($C_{17}H_{15}FN_2O$) C, H, N.

Crystal structure of **13** has been proven by X-ray analysis: CAD4 Enraf Nonius, Cu Kα, SIR-92, SHELXL-97. Further details of the crystal structure analysis are available in the references.[22]

1-(4-Fluorophenyl)-2-(4-pyridin) Ethanone (14). Diisopropylamine (138 mmol) in THF (150 mL) was cooled to −78 °C under argon, *n*-butyl lithium (1.6 M, 50 mL) was added, and the mixture was stirred for 1 h (preparation of LDA). Picoline (92 mmol) in THF was added dropwise, and after 1 h, 4-fluoro-*N*-methoxy-*N*-methylbenzamide (92 mmol) in THF was added and the reaction was then warmed to 0 °C over a period of 2 h. Brine (50 mL) was added, and the mixture was extracted by diethyl ether (200 mL). The organic phase was separated, dried over Na_2SO_4, and evaporated. The oily orange-brown product was purified by column chromatography using DCM 95/ethanol 5 to yield 39% of compound **14**: mp = 91.4 °C. ^{1}H NMR ($CDCl_3$, 200 MHz, ppm): δ 4.27 (s, 2H, CH_2), 7.1−7.2 (m, 4H, CHAr), 8.0 (m, 2H, CHAr), 8.6 (d, 2H, CHAr).

4-[3-(4-Fluorophenyl)-5-phenylisoxazol-4-yl]pyridine (15). (a) Amounts equal to 21.5 g (100 mmol) of compound **14**, sodium acetate (36.1 g, 440 mmol), hydroxylamine HCl (22.0 g, 320 mmol), and 250 mL 50% methanol/water were refluxed for 1.5 h. By cooling in an ice bath, the product precipitated as a solid, which was filtered, washed with water, and dried over P_2O_5 (yield 90%). A sample of 1-(4-fluorophenyl)-2-(4-pyridin) ethanone oxime was analyzed: mp = 137.6 °C; MS +c Full ms (*m*/*z*) 230 (M^+). ^{1}H

NMR ($CDCl_3$, 200 MHz, ppm): δ 4.21 (s, 2H), 7.0 (m, 2H), 7.24 (d, 2H), 7.6 (m, 2H), 8.5 (d, 2H), 9.85 (br s, 1H).

(b) An aliquot of 2.3 g (10 mmol) of 1-(4-fluorophenyl)-2-(4-pyridin) ethanone oxime in 100 mL of DCM was cooled in an ice bath and 3.0 g (30 mmol) of triethylamine was added. After 1 h, hydroxybenzenecarboximidoyl chloride (3.1 g, 20 mmol) was dropped, and the reaction mixture was allowed to stir at rt over 12 h. The solid (triethylamine HCl) was filtered, and the organic phase was evaporated in vacuum. The residue was purified by column chromatography using DCM 97.5/ethanol 2.5 to yield 17% of compound **15**: mp = 197.7 °C; MS +c Full ms (*m*/*z*) 316.0 (M^+). ^{1}H NMR ($CDCl_3$, 200 MHz, ppm): δ 7.0−7.2 (m, 4H), 7.38−7.42 (m, 5H), 7.49−7.54 (m, 2H), 8.63−8.67 (dd, 2H).

4-[5-(4-Fluorophenyl)-3-isopropylisoxazol-4-yl]pyridine (16). An amount equal to 3.8 mmol of **14** was reacted for 1 h at −78 °C with 15.2 mmol of LDA. Then 15.2 mmol of isobutyryl chloride oxime in THF was added, and the reaction mixture was stirred for 3 h at −78 °C, then allowed to warm to rt. Water was added carefully, and the mixture was extracted with ethyl acetate (200 mL). The organic phase was separated, dried over Na_2SO_4, and evaporated to yield an orange oil that was purified by column chromatography (ethyl acetate/hexanes 4/6) to yield 40% of **16** as a white solid: mp = 100.5 °C; MS +c Full ms (*m*/*z*) 282.1 (M^+). ^{1}H NMR ($CDCl_3$, 200 MHz, ppm): δ 1.25 (s, 3H), 1.28 (s, 3H), 2.97 (m, 1H), 7.03 (m, 2H), 7.25 (d, 2H), 7.45 (m, 2H), 8.7 (d, 2H). ^{13}C NMR ($CDCl_3$, 200 MHz, ppm): δ 21.2 (CH_3), 26.0 (CH), 112.5 (C_q), 115.7 (CH), 116.2 (CH), 123.4 (CH), 124.8 (CH), 128.8 (CH), 129.1 (CH), 139.5 (C_q), 150.6 (CH), 161 (C_q), 164.3 (C_q), 166.0 (C_q), 167.64 (C_q). Anal. ($C_{17}H_{15}FN_2O$) C, H, N.

Crystal structure of **16** has been proven by X-ray analysis: CAD4 Enraf Nonius, Cu Kα, SIR-92, SHELXL-97. Further details of the crystal structure analysis are available in the references.[23]

Biological Evaluation. The p38αMAPK[24] and JNK3[25] in vitro assays to determine biological activity of test compounds were performed according to the published procedure. The IC_{50} values were measured by testing four concentrations of compounds at least 6-fold. The final DMSO concentration in the assay was 1%. Statistical data can be found in Supporting Information.

Molecular Modeling. All modeling was performed on a redhat Enterprise Linux system. SYBYL 7.2 (Tripos, Inc.) was used to build, minimize, visualize, or measure the distances and angles of the structures. All modeling graphics were created with "The Gimp" (version 1.2.3).

The distances and bond angles of **5**, **10**, **13**, and **16** were determined by measuring the X-ray based crystal structures with the "analyze-distance and angle-tool" of SYBYL 7.2. The deviations between build up and minimized structures, which were created with the "Build/Edit-Get Fragment" tool and the crystallized structures pertain to the second decimal place.

Structure of **17** was calculated by the following method: structure was built from fragments of the Sybyl database, minimized with MMFF94 (method, conj. grad.; initial optimization, "None"; termination gradient, 0.05 kcal/(mol Å)) and then measured with the "analyze-distance and angle-tool".

Structures of **5**, **10**, **13**, and **16** were docked into the X-ray protein structures of JNK3 (pdb code 1pmq[35]) and p38α (pdb code 1oz1[36]) using FlexiDock implemented in Sybyl 7.2. The charges of the ligands were determined with MMFF94, while the charges of the protein structures were calculated by using AmberFF02 after deleting the water molecules. The binding pocket was defined as the residues in radius of 5 Å surrounding the ligand of the original pdb structures. No H-bond sites were marked. All bonds connected to the 5- and 6-membered rings of the ligand were treated as rotatable during the docking process. In the case of p38α, the side chains of Met109, Thr106, and Lys53 were treated as flexible, as in JNK3 Met146, Met149, and Lys93, respectively. The volumes of key residues Thr106/p38α and Met146/JNK3 were determined in each case from two protein X-ray structures pdb codes 1w84[37] and 10z1[36] for p38α (Thr106 = 3687.29 Å^3 ± 30.65); 1pmn and 1pmq[35] for JNK3 (Met146 = 3970.01 ± 34.28 Å^3) as the average values.

Overlay of p38α (cyan, pdb code 1a9u,[16] which includes **20**) and JNK3 (dark blue, pdb code 1pmn[35]) occurs by homology aligning in a capped stick illustration (biopolymer-align structures by homology).

Acknowledgment. We are grateful to Dr. W. Zimmermann for the synthesis of compound **17**. Financial support by Merckle GmbH Blaubeuren, DAAD, and Fonds der Chemischen Industrie is gratefully acknowledged.

Supporting Information Available: IR and CHN analysis data for compounds. Statistical data for biological assays. This material is available free of charge via the Internet at http://pubs.acs.org.

References

(1) Kung, C.; Shokat, K. M. Small-molecule kinase-inhibitor target assessment. *ChemBioChem* **2005**, *6*, 523−526.
(2) Hopkins, A. L.; Groom, C. R. The druggable genome. *Nat. Rev. Drug Discovery* **2002**, *1*, 727−730.
(3) Manning, G.; Whyte, D. B.; Martinez, R.; Hunter, T.; Sudarsanam, S. The protein kinase complement of the human genome. *Science* **2002**, *298*, 1912−1916.
(4) Milanesi, L.; Petrillo, M.; Sepe, L.; Boccia, A.; D'Agostino, N.; Passamano, M.; Di Nardo, S.; Tasco, G.; Casadio, R.; Paolella, G. Systematic analysis of human kinase genes: a large number of genes and alternative splicing events result in functional and structural diversity. *BMC Bioinformatics* **2005**, *6 Suppl 4*, 20.
(5) Daub, H. Characterization of kinase-selective inhibitors by chemical proteomics. *Biochim. Biophys. Acta* **2005**, *1754*, 183−190.
(6) Luo, Y. Selectivity assessment of kinase inhibitors: Strategies and challenges. *Curr. Opin. Mol. Ther.* **2005**, *7*, 251−255.
(7) Ortiz, A. R.; Gomez-Puertas, P.; Leo-Macias, A.; Lopez-Romero, P.; Lopez, V.; Morreale, A.; Murcia, M.; Wang, K. Computational approaches to model ligand selectivity in drug design. *Curr. Top. Med. Chem.* **2006**, *6*, 41−55.
(8) Knight, Z. A.; Shokat, K. M. Features of selective kinase inhibitors. *Chem. Biol.* **2005**, *12*, 621−637.
(9) Richards, M. L. Hot topic: New approaches to the treatment of inflammatory disorders. *Curr. Top. Med. Chem.* **2006**, *6*, 75.
(10) McGovern, S. L.; Shoichet, B. K. Kinase inhibitors: Not just for kinases anymore. *J. Med. Chem.* **2003**, *46*, 1478−1483.
(11) Boldt, S.; Kolch, W. Targeting MAPK signalling: Prometheus' fire or pandora's box? *Curr. Pharm. Des.* **2004**, *10*, 1885−1905.
(12) Manning, A. M.; Davis, R. J. Targeting JNK for therapeutic benefit: From junk to gold? *Nat. Rev. Drug Discovery* **2003**, *2*, 554−565.
(13) Johnson, G. L.; Lapadat, R. Mitogen-activated protein kinase pathways mediated by ERK, JNK, and p38 protein kinases. *Science* **2002**, *298*, 1911−1912.
(14) (a) Choo, M. K.; Sakurai, H.; Koizumi, K.; Saiki, I. TAK1-mediated stress signaling pathways are essential for TNF-α-promoted pulmonary metastasis of murine colon cancer cells. *Int. J. Cancer* **2006**, *118*, 2758−2764. (b) Argast, G. M.; Fausto, N.; Campbell, J. S. Inhibition of RIP2/RICK/CARDIAK activity by pyridinyl imidazole inhibitors of p38 MAPK. *Mol. Cell. Biochem.* **2005**, *268*, 129−140. (c) Harper, S. J.; LoGrasso, P. Inhibitors of the JNK signaling pathway. *Drugs Future* **2001**, *26*, 957−973.
(15) Goldstein, D. M.; Gabriel, T. Pathway to the clinic: Inhibition of P38 MAP kinase. A review of ten chemotypes selected for development. *Curr. Top. Med. Chem.* **2005**, *5*, 1017−1029.
(16) (a) Lantos, I.; Bender, P. E.; Razgaitis, K. A.; Sutton, B. M.; DiMartino, M. J.; Griswold, D. E.; Walz, D. T. Antiinflammatory activity of 5,6-diaryl-2,3-dihydroimidazo[2,1-*b*]thiazoles. Isomeric 4-pyridyl and 4-substituted phenyl derivatives. *J. Med. Chem.* **1984**, *27*, 72−75. (b) Wang, Z.; Canagarajah, B. J.; Boehm, J. C.; Kassisa, S.; Cobb, M. H.; Young, P. R.; Abdel-Meguid, S.; Adams, J. L.; Goldsmith, E. J. Structural basis of inhibitor selectivity in MAP kinases. *Structure* **1998**, *6*, 1117−1128.
(17) Wagner, G.; Laufer, S. Small molecular anti-cytokine agents. *Med. Res. Rev.* **2006**, *26*, 1−62.
(18) Peifer, C.; Wagner, G.; Laufer, S. New approaches to the treatment of inflammatory disorders by small molecule inhibitors of p38 MAP kinase. *Curr. Top. Med. Chem.* **2006**, *6*, 113−149.
(19) Fricker, M.; LoGrasso, P.; Ellis, S.; Wilkie, N.; Hunt, P.; Pollack, S. J. Substituting c-Jun N-terminal kinase-3 (JNK3) ATP-binding site amino acid residues with their p38 counterparts affects binding of JNK- and p38-selective inhibitors. *Arch. Biochem. Biophys.* **2005**, *438*, 195−205.
(20) Peifer, C.; Schollmeyer, D.; Laudage, S.; Laufer, S. 3-(4-Fluorophenyl)-4-(4-pyridyl)quinolin-2(1*H*)-one. *Acta Crystallogr., Sect. E: Struct. Rep. Online* **2006**, *62*, 2475−2477.

(21) Peifer, C.; Schollmeyer, D.; Selig, R.; Laufer, S. 4-(4-Fluorophenyl)-3-(4-pyridyl)quinolin-2(1*H*)-one. *Acta Crystallogr., Sect. E: Struct. Rep. Online* **2006**, *62*, 2648−2650.
(22) Peifer, C.; Abadleh, M.; Schollmeyer, D. Laufer, S. 4-[3-(4-Fluorophenyl)-5-isopropylisoxazol-4-yl]pyridine. *Acta. Crystallogr., Sect. E: Struct. Rep. Online* **2006**, *62*, 3707−3709.
(23) Peifer, C.; Abadleh, M.; Schollmeyer, D.; Laufer, S. 5-[(4-Fluorophenyl)-3-isopropylisoxazol-4-yl]pyridine. *Acta Crystallogr., Sect. E: Struct. Rep. Online* **2006**, *62*, 3647−3649.
(24) Laufer, S.; Thuma, S.; Peifer, C.; Greim, C.; Herweh, Y.; Albrecht, A.; Dehner, F. An immunosorbent, nonradioactive p38 MAP kinase assay comparable to standard radioactive liquid-phase assays. *Anal. Biochem.* **2005**, 135−137.
(25) Peifer, C.; Luik, S.; Thuma, S.; Herweh, Y.; Laufer, S. Development and optimization of a non-radioactive JNK3 assay. *Comb. Chem. High Throughput Screening* **2006**, *9*, 613−618.
(26) Wagner, G. K. Pyridinyl-pyrimidine- und imidazole-Neue Hemmstoffe der Zytokinfreisetzung. Ph.D. Dissertation, Universität Tübingen, Tübingen, Germany, 2003.
(27) McIntyre, C. J.; Ponticello, G. S.; Liverton, N. J.; O'Keefe, S. J.; O'Neill, E. A.; Pang, M.; Schwartz, C. D.; Claremon, D. A. Pyridazine based inhibitors of p38 MAPK. *Bioorg. Med. Chem. Lett.* **2002**, *12*, 689−692.
(28) Kadnikov, D. V.; Larock, R. C. Synthesis of 2-quinolones via palladium-catalyzed carbonylative annulation of internal alkynes by *N*-substituted *o*-iodoanilines. *J. Org. Chem.* **2004**, *69*, 6772−6780.
(29) Fürstner, A.; Hupperts, A. Carbonyl coupling reactions catalytic in titanium and the use of commercial titanium powder for organic synthesis. *J. Am. Chem. Soc.* **1995**, *117*, 4468−4475.
(30) Cho, I. S.; Gong, L.; Muchowski, J. M. Synthesis of quinolines via *ortho*-lithiated *N*-acylanilines. A modified Friedlander synthesis. *J. Org. Chem.* **1991**, *56*, 7288−7291.
(31) Chai, K. B.; Sampson, P. A convenient and efficient three-step synthesis of α-chloro keto acids. *Tetrahedron Lett.* **1992**, *33*, 585−588.
(32) Marcaccini, S.; Pepino, R.; Pozo, M. C.; Basurto, S.; Valverde, M.; Torroba, T. One-pot synthesis of quinolin-2-(1*H*)-ones via tandem Ugi-Knoevenagel condensations. *Tetrahedron Lett.* **2004**, *45*, 3999−4001.
(33) Rupert, K. C.; Henry, J. R.; Dodd, J. H.; Wadsworth, S. A.; Cavender, D. E.; Olini, G. C.; Fahmy, B.; Siekierka, J. J. Imidazopyrimidines, potent inhibitors of p38 MAP kinase. *Bioorg. Med. Chem. Lett.* **2003**, *13*, 347−350.
(34) Micetich, R. G.; Shaw, C. C.; Hall, T. W.; Spevak, P.; Fortier, R. A.; Wolfert, P.; Foster, B. C.; Bains, B. K. The 5-alkoxymethyl-, 5-alkylthiomethyl-, and 5-dialkylaminomethylisoxazoles. *Heterocycles* **1985**, *23*, 571−583.
(35) Scapin, G. Structural biology in drug design: Selective protein kinase inhibitors. *Drug Discovery Today* **2002**, *7*, 601−611.
(36) Trejo, A.; Arzeno, H.; Browner, M.; Chanda, S.; Cheng, S.; Comer, D. D.; Dalrymple, S. A.; Dunten, P.; Lafargue, J.; Lovejoy, B.; Freire-Moar, J.; Lim, J.; McIntosh, J.; Miller, J.; Papp, E.; Reuter, D.; Roberts, R.; Sanpablo, F.; Saunders, J.; Song, K.; Villasenor, A.; Warren, S. D.; Welch, M.; Weller, P.; Whiteley, P. E.; Zeng, L.; Goldstein, D. M. Design and synthesis of 4-azaindoles as inhibitors of p38 MAP kinase. *J. Med. Chem.* **2003**, *46*, 4702−4713.
(37) Gill, A. L.; Frederickson, M.; Cleasby, A.; Woodhead, S. J.; Carr, M. G.; Woodhead, A. J.; Walker, M. T.; Congreve, M. S.; Devine, L. A.; Tisi, D.; O'Reilly, M.; Seavers, L. C.; Davis, D. J.; Curry, J.; Anthony, R.; Padova, A.; Murray, C. W.; Carr, R. A.; Jhoti, H. Identification of novel p38α MAP kinase inhibitors using fragment-based lead generation. *J. Med. Chem.* **2005**, *48*, 414−426.

JM061097O